Science of the Total Environment 660 (2019) 177–187

Contents lists available at ScienceDirect

Science of the Total Environment

journal homepage: www.elsevier.com/locate/scitotenv

Impacts of Chinese Grain for Green program and climate change on vegetation in the Loess Plateau during 1982–2015

Gang Li [a,b,c,d], Shaobo Sun [e,*], Jichang Han [a,b,c,d], Jianwu Yan [f,g], Wenbin Liu [h], Yang Wei [a,b,c,d], Nan Lu [a,b,c,d], Yingying Sun [a,b,c,d]

[a] Shaanxi Provincial Land Engineering Construction Group Co., Ltd., Xi'an 710075, China
[b] Key Laboratory of Degraded and Unused Land Consolidation Engineering, the Ministry of Land and Resources of China, Xi'an 710075, China
[c] Shaanxi Provincial Land Construction Engineering Technology Research Center, Xi'an 710075, China
[d] Institute of Land Engineering and Technology, Shaanxi Provincial Land Engineering Construction Group Co., Ltd., Xi'an 710075, China
[e] Institute of Surface-Earth System Science, Tianjin University, Tianjin 300072, China
[f] School of Geography and Tourism, Shaanxi Normal University, Xi'an 710119, China
[g] National Demonstration Center for Experimental Geography Education, Shaanxi Normal University, Xi'an 710119, China
[h] Key Laboratory of Water Cycle and Related Land Surface Processes, Institute of Geographical Sciences and Natural Resources Research, Chinese Academy of Sciences, Beijing 100101, China

HIGHLIGHTS

- The Grain for Green Program (GGP) greatly changed vegetation in the Loess Plateau.
- Climate changes exerted adverse effects on vegetation in the LP before the GGP.
- Wetting and reduced drought positively affected vegetation in the LP after the GGP.
- The inter-annual variation of NDVI was primarily determined by soil moisture.

GRAPHICAL ABSTRACT

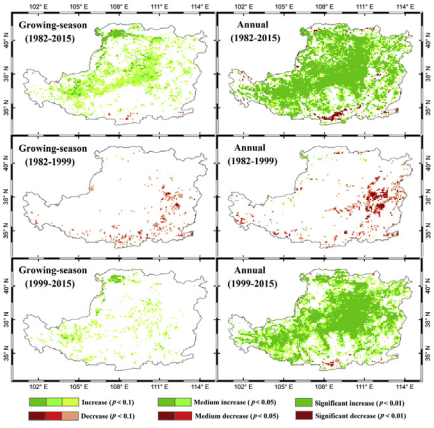

ARTICLE INFO

Article history:
Received 24 October 2018
Received in revised form 8 December 2018
Accepted 4 January 2019
Available online 5 January 2019

Editor: Ashantha Goonetilleke

Keywords:
Normalized difference vegetation index (NDVI)
Climate change
Loess Plateau
Grain for Green Program (GGP)

ABSTRACT

Remote sensing based vegetation index provides a practical method for the monitoring of vegetation dynamics at regional and global scales. Here, using a long-term remotely sensed normalized difference vegetation index (NDVI) dataset, we quantified the vegetation changes in the Loess Plateau (LP) over the last three decades (1982–2015), which includes the period before the Chinese"Grain for Green Program"(GGP) was launched (1982–1999), and the period after the GGP (1999–2015). The correlations between the NDVI and four climate related variables, i.e., precipitation, temperature, root-soil moisture (RSM), and a drought proxy-standardized evapotranspiration deficit index (SEDI), were also examined. The results indicated that, (i) the GGP strongly changed the vegetation in the LP. The growing-season mean NDVI (GSM-NDVI) and the annual mean NDVI (AM-NDVI) decreased slightly before the GGP launched in 1999, with slopes of -3.38×10^{-3} and -8.00×10^{-4} year^{-1}, respectively. However, they showed slight and significant ($p < 0.05$) increases after the GGP, with slopes of 4.75×10^{-3} and 2.32×10^{-3} year^{-1}, respectively. (ii) Climate change

* Corresponding author at: No. 92 Weijin Road, Nankai District, Tianjin 300072, China.
E-mail address: shaobo.sun@tju.edu.cn (S. Sun).

https://doi.org/10.1016/j.scitotenv.2019.01.028

Drought
Remote sensing

(i.e., warming and drying) resulted in adverse effects on vegetation in the LP during the period before the GGP. However, the observed changes (i.e., wetting and reduced drought) exerted positive effects on the vegetation during the period after the GGP. (iii) Inter-annual variations of spatially averaged NDVI over the LP were primarily determined by RSM rather than any other climate related variables. In the southeastern LP, the inter-annual variation of GSM-NDVI was mainly determined by precipitation and SEDI, while the inter-annual variation of AM-NDVI was mainly caused by SEDI and RSM. Inter-annual variations of both GSM-NDVI and AM-NDVI were mainly determined by SEDI and RSM in the northwestern LP, and by temperature in the southwestern LP.

1. Introduction

The Loess Plateau (LP) of China is located in the middle reaches of the Yellow River and covers an area of 6.4×10^5 km^2. Historically (before 8 CE), the LP was covered by forests and grassland (Fang and Xie, 1994). However, due to strong human activities (deforestation) and climate change, it suffered from several severe environmental problems in the last century, such as, soil erosion and severe water shortage (Zheng et al., 2005; Zheng, 2006; Zhao et al., 2013; Jin et al., 2017a).

To address these severe environmental problems, the Chinese government has implemented several afforestation programmes over the past several decades (Yuan et al., 2014). The Grain for Green Program (GGP) launched in 1999 is the largest such program and aims to increase the forest cover and to mitigate soil erosion by converting agricultural lands on steep slopes to either forests or grasslands (Xiao, 2014; Feng et al., 2016; S. Wang et al. 2017). The LP is the most representative region for the implementation of the GGP. With large investment, the vegetation cover of the LP has increased by 25% over the last decades (Feng et al., 2016).

Satellite remote sensing provides the best practical mean to monitor vegetation dynamics at both regional and global scales (Forzieri et al., 2017; X. Wang et al. 2017; Song et al., 2018; Tong et al., 2018). Over the past several years and with the help of multiple remote sensing data, many researchers have investigated the vegetation dynamics in the LP and the vegetation responses to the changing climate (Yuan et al., 2014; Li et al., 2014; Xiao, 2014; Li et al., 2015; Feng et al., 2016; Guo and Gong, 2016; Chen et al., 2017; Jin et al., 2017b; Li et al., 2017; Y. Wang et al. 2017; Yang et al., 2017; Zhang et al., 2017; Zhao et al., 2018). For example, using remotely sensed normalized-difference vegetation index (NDVI) data, Li et al. (2014) assessed the vegetation dynamics in the southwest LP over 1981–2010 and analyzed the correlations between the vegetation and climate variables (temperature, net radiation, and precipitation). Based on multiple Moderate Resolution Imaging Spectroradiometer (MODIS) products, Xiao (2014) quantified vegetation changes and their biophysical consequences for the years after the launch of the GGP (2000—2013). Li et al. (2015) analyzed the spatio-temporal characteristics of vegetation and their relationship with changes of climate (temperature and precipitation) and human activities on the LP for 2000–2014. Li et al. (2017) examined the changes of vegetation coverage in the LP over 1982–2015 and analyzed the impacts of precipitation, temperature, elevation, and slope on the vegetation. Zhao et al. (2018) assessed the impact of drought on vegetation productivity in the LP over 1981–2013. However, when investigating the impacts of climate change on vegetation, most of these studies focused on the effects of inter-annual variations of precipitation and temperature. Few studies have synthetically considered the effects of precipitation, temperature, and other important environmental factors such as soil moisture and drought. Compared to precipitation, soil moisture exerts a more direct effect on vegetation growth, and is largely determined by soil properties, topography, and other land surface features. For arid and semi-arid regions (such as the LP), vegetation is frequently affected by drought, especially during the growing season. Therefore, when investigating the impacts of climate change on vegetation, not only environmental factors such as precipitation and temperature, but also soil moisture, drought, and other important factors should be considered, especially for arid and semi-arid regions (Zhang et al., 2015). Moreover, the analyses should also be conducted at the growing-season scale rather than only at the annual scale, since vegetation is more sensitive to changes of climate during growing season than the year as a whole.

In this study, regarding NDVI as a proxy of vegetation, the vegetation dynamics in the LP were assessed over the last three decades (1982–2015), which includes the period before the GGP (1982–1999) and the period after the GPP (1999–2015), during growing-season (Apr. to Oct.) and at annual scale. The correlations between the NDVI and several climatic variables (precipitation, temperature, soil moisture, and drought) were analyzed. The sensitivities of the NDVI variations to the climatic variables were also examined.

2. Materials and methods

2.1. Study area

The LP is located in north China and covers an area of approximately 6.4×105 km^2 (Fig. 1). It covers the entirety of Ningxia and Shanxi, most of Shannxi, and portions of Henan, Inner Mongolia, Gansu, and Qinghai provinces. The mean annual temperature (MAT) of the LP ranges from 3.7 to 14.0 °C, and the mean annual precipitation (MAP) ranges within 144–812 mm (Li et al., 2010; Xiao, 2014). The types of land cover mainly include cropland, grassland, forest, bare land, and urban and built-up land. Cropland, grassland, and forest accounted for 89% of the total area of the LP in 2010 (Li et al., 2016). Overall, the vegetation decreases from southeastern to northwestern regions. In the northwestern LP, the land cover types are mainly cropland and bare land, while in the southeastern LP the main land cover types are cropland and forest.

2.2. Data description and preprocessing

The NDVI data derived from the Advanced Very High Resolution Radiometer (AVHRR) was used to quantify the vegetation changes and analyze their correlations with variables related to climate in the LP. The AVHRR based NDVI was developed by the Global Inventory Modeling and Mapping Studies (GIMMS) group (Tucker et al., 2005). It has several advantages, including well considering the calibration loss, orbital drift, and volcanic eruptions (X. Wang et al. 2017). It currently covers the period from 1981 (Jul. 1981) to 2015, and has spatial and temporal resolutions of 8 km and 15 days, respectively.

The precipitation and temperature data were obtained from the China Meteorological Data Service Center (http://data.cma.cn/en). These data produced by interpolating the observations from 2472 China meteorological stations beginning in 1961. The spatial and temporal resolutions were 0.5° × 0.5°and monthly, respectively.

The soil moisture data was obtained from the Global Land Evaporation Amsterdam Model (GLEAM) root-zone soil moisture (RSM) dataset (version 3.2a) (Martens et al., 2017), which is a global soil moisture data set that was developed based on multiple satellite data and a data assimilation system. It currently covers a period of 1980–2017, has a spatial resolution of 0.25° × 0.25°, and a daily temporal resolution. It has

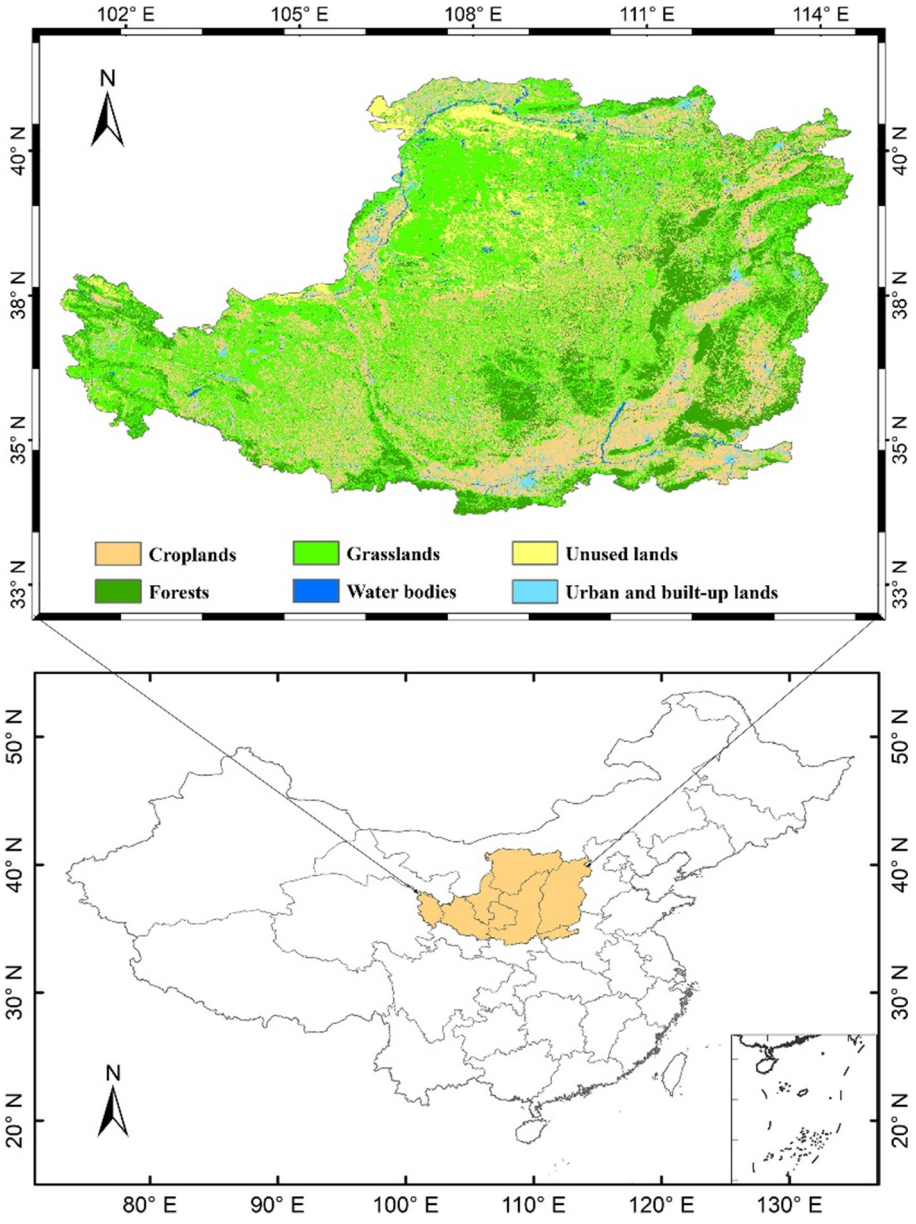

Fig. 1. Location and land cover types of the Loess Plateau. The base map is from the China 1 km land cover data (2015) (Liu et al., 2005).

been globally validated against 2325 measurements across a broad range of ecosystems, and has been widely used in recent studies (Miralles and Teuling, 2014; Guillod et al., 2015). More details about this data can be found in Martens et al. (2017) and on the website (https://www.gleam.eu/).

Here, the standardized evapotranspiration deficit index (SEDI) was used as a proxy of drought. The SEDI data was obtained from the GLEAM land datasets. It has a spatial resolution of 0.25° × 0.25°, covers a period of 1980–2016, and has a monthly temporal interval. Because the SEDI was missing for most land of the LP in Dec., the annual mean SEDI was calculated as the average of SEDI from Jan. to Nov. More detail about this dataset can be find in Vicente-Serrano et al. (2018).

When analyzing the relationships between NDVI and climatic variables, all NDVI and climate related data sets (if necessary) were aggregated or reggrided to a spatial resolution of 0.25° × 0.25°.

2.3. Methods

The linear least-square regression method was used to determine the trend of the spatially averaged NDVI in the LP. An *F* test was used to examine the statistical significance of the trends. To compare the patterns of the variations in NDVI and climate related variables, the spatial distributions of the trends of NDVI and each climate related variable were also analyzed.

The nonparametric Mann-Kendall (M-K) test (Kendall, 1975; Mann, 1945) was used to determine the NDVI trends and to quantify their statistical significance at the pixel scale. According to the Z-values from M-K test, the NDVI pixels were divided into seven classes: significant decrease (Z-value < −2.32, with $p < 0.01$); medium decrease (Z-value < −1.96, with $p < 0.05$); decrease (Z-value < −1.65, with $p < 0.1$); not significant (|Z-value| < 1.65); increase (Z-value > 1.65, with $p < 0.1$); medium increase (Z-value > 1.96, with $p < 0.05$); and significant increase (Z-value > 2.32, with $p < 0.01$) (Sun et al., 2018).

We used the multiple linear regression approach to diagnose the sensitivities of the inter-annual variation of NDVI to the climate related variables. The relevant formula is:

$$y = \gamma_{pre} \times P + \delta_{tem} \times T + \varphi_{SM} \times SM + \psi_{SEDI} \times SEDI + \varepsilon \quad (1)$$

where y is the spatially averaged NDVI; P, T, SM, and $SEDI$ represent the spatially averaged precipitation, temperature, RSM, and SEDI, respectively. All variables, including y were normalized (Eq. (2)). γ_{pre}, δ_{tem}, φ_{SM}, and ψ_{SEDI} are the fitted regression coefficients and ε is the residual error term. As reported by previous studies (Piao et al., 2013; Sun et al., 2018), although γ_{pre}, δ_{tem}, φ_{SM}, and ψ_{SEDI} are not the true sensitivities of the dependent variable (NDVI) to the independent variables (climatic variables), they can be regarded as apparent sensitivities and can be used to represent the contributions of the variations of independent variables to dependent variable.

$$z_i = \frac{x_i - \bar{x}}{\sigma} \tag{2}$$

where x_i is the NDVI or climate variables in the ith year. $\bar{x}$ and σ are the mean and standard deviation (SD) of variable x, respectively. z_i is the normalized x in the ith year.

Precipitation, temperature, soil moisture, and drought were considered as major climatic variables that directly affect vegetation growth. Because these four variables may be well correlated (e.g., precipitation and soil moisture), a linear correlation analysis was not suitable to analyze and compare their impacts on NDVI. Here, we used the partial correlation analysis (Eq. (3)) to quantify the effects of the inter-annual variation of one climatic variable on that of the NDVI after statistically controlling changes in the others.

$$r_{i,j-l_1 l2\ldots l_n} = \frac{r_{i,j-l_1 l2\ldots l_{n-1}} - r_{i,l_n-l_1 l2\ldots l_{n-1}} \cdot r_{j,l_n-l_1 l2\ldots l_{n-1}}}{\sqrt{\left(1-r^2_{i,l_n-l_1 l^2\ldots l_{n-1}}\right)\left(1-r^2_{j,l_n-l_1 l^2\ldots l_{n-1}}\right)}} \tag{3}$$

where $r_{i,j-l_1 l2\ldots l_n}$ represents the nth ($n \le k$-2) order partial correlation coefficient between x_i and x_j, k represents the number of the variables. Each term on the right of Eq. (3) represents the $(n-1)$ th order partial correlation coefficient. A t-test (Eq. (4)) was used to examine the statistical significance of the partial correlation coefficient, and a p-value < 0.05 was considered as significant level.

$$t = \frac{\sqrt{m-k-2} \cdot r_{i,j-l_1 l2\ldots l_n}}{\sqrt{1\text{-}r^2_{i,j-l_1 l^2\ldots ln}}} \tag{4}$$

where m represents the number of samples.

3. Results

3.1. NDVI patterns and climate related variables

Fig. 2 shows the spatial distributions of the annual mean NDVI (AM-NDVI) and the growing season mean NDVI (GSM-NDVI) and their SD for 1982–2015. The NDVI in the LP ranged from 0.07 to 0.72, with spatially averaged GSM-NDVI and AM-NDVI of 0.33 ± 0.07 and 0.32 ± 0.02, respectively. The patterns of GSM-NDVI and AM-NDVI were similar, decreasing from the southeastern to the northwestern LP. In the southeastern LP, both the GSM-NDVI and AM-NDVI showed large spatial variability, which is consistent with the land use types (Fig. 1). Overall, the forest regions in the southeast had the largest NDVI (>0.5), followed by the southeastern croplands (0.3–0.5), and grasslands (<0.3) in the southwest. The spatial distributions of the SD of the NDVI data suggest that the inter-annual variations of GSM-NDVI were significantly larger than that of AM-NDVI, especially in the central, southeastern, and western LP.

The patterns of annual and growing-season precipitation were similar to that of the NDVI (Fig. S1) and showed a clear decreasing gradient from the southeastern to northwestern LP. The growing-season mean temperature was significantly higher than the annual mean temperature. Except for small regions in the western and southern LP, both the annual mean and the growing season mean temperature showed relatively small spatial variations compared to the precipitation. The patterns of annual mean and growing-season mean RSM were very

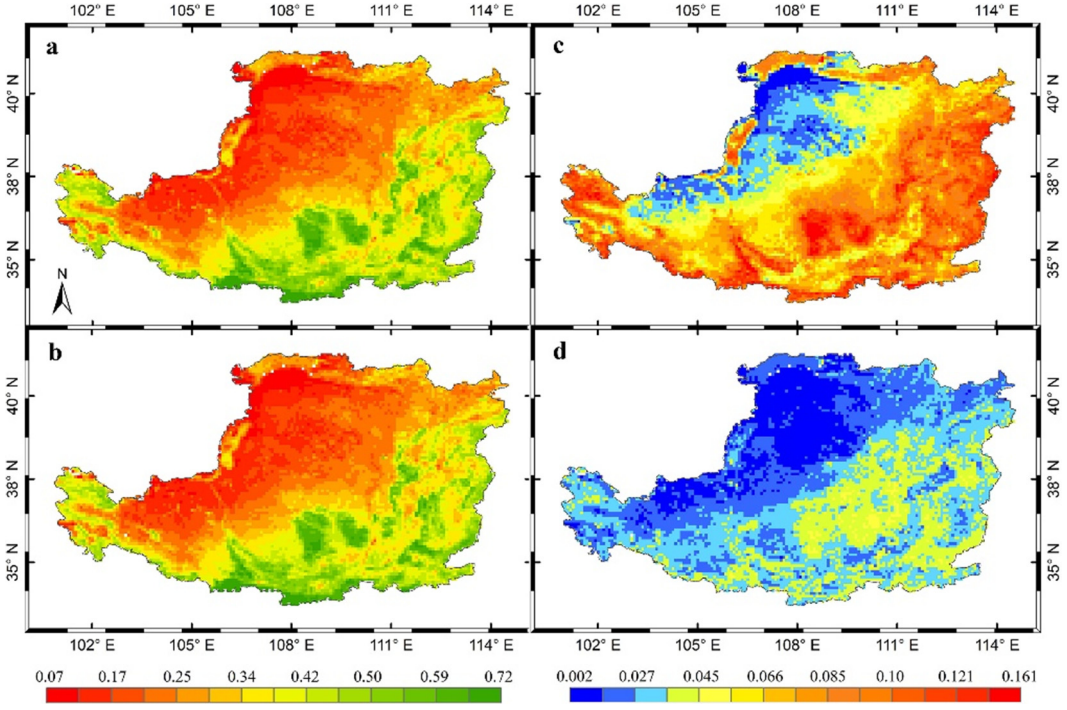

Fig. 2. The spatial distributions of GSM-NDVI (a) and AM-NDVI (b) as well as their standard deviation (c and d) in the LP for 1982–2015.

similar to that of the corresponding precipitation, showing a decrease from the southeastern LP to northwestern LP. The highest RSM in the southeastern LP was >0.25 and the lowest RSM in the northwestern LP was <0.20. As expected, the patterns of SEDI agreed well with RSM and precipitation, decreasing from the northwest to southeast, which indicates that the high vegetation regions in the southeastern LP may suffer larger drought than the western and northern LP.

3.2. Spatio-temporal variations of NDVI in the LP

The spatially averaged AM-NDVI in the LP showed a significant and positive trend over 1982–2015 ($p < 0.05$), with a value of 8.72×10^{-4} year^{-1}, indicating that the vegetation significantly increased in the LP over the last three decades (Fig. 3b). The GSM-NDVI had a positive but not significant trend ($p < 0.05$), with a value of 1.67×10^{-3} year^{-1} (Fig. 3a). Before the GGP was launched in 1999, both the AM-NDVI and GSM-NDVI were slightly, but not significantly decreased ($p < 0.05$), with slopes of 8.00×10^{-4} and -3.38×10^{-3} year^{-1}, respectively. After launch of the GGP, the trends of the NDVI became positive. The spatially averaged AM-NDVI and GSM-NDVI significantly and slightly increased with slope values of 2.32×10^{-3} year^{-1} and 4.75×10^{-3} year^{-1}, respectively.

The MK-based changes in NDVI clearly indicate that the GGP significantly changed the vegetation in the LP over the past three decades (Fig. 4). 43.4% (3.5%), 53.4% (11.5%), and 61.8% (26.6%) of the LP showed significantly increased, medium increased, and increased AM-NDVI (GSM-NDVI) over 1982–2015, respectively. In contrast, only 1.2% (0.04%), 1.6% (0.14%), and 2.3% (0.25%) of the LP showed significantly decreased, medium decreased, and decreased AM-NDVI (GSM-NDVI), respectively. The increasing NDVI were mostly distributed in the northwestern LP, and the decreasing NDVI were mainly found in small regions in the southern LP.

Before the GGP was launched in 1999, except for small regions in the eastern and southern LP suffered decreasing NDVI, most regions of the LP showed relatively stable GSM-NDVI and AM-NDVI without significant changes. 1.2% (0.1%), 3.5% (0.9%), and 8.1% (4.1%) of the LP showed significantly decreased, medium decreased, and decreased AM-NDVI (GSM-NDVI) over 1982–1999, respectively. Almost no area showed an increasing NDVI (<0.05%).

Fig. 4c&f shows that the GGP strongly changed the NDVI trends over the LP. 34.5% (0.8%), 47.3% (2.2%), and 59.2% (8.5%) of LP showed significantly increased, medium increased, and increased AM-NDVI (GSM-NDVI) over 1999–2015, respectively. Almost no regions showed decreasing NDVI (<0.8%). The increasing AM-NDVI

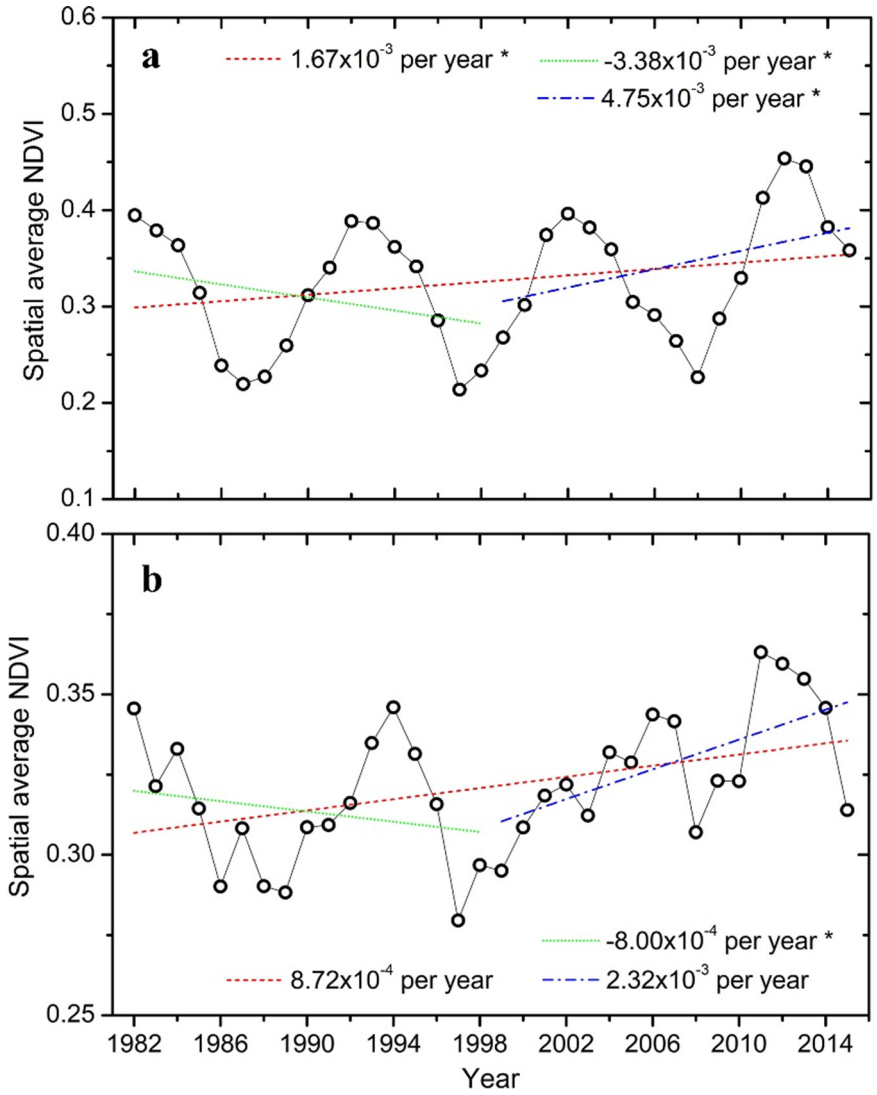

Fig. 3. Inter-annual variations of spatially averaged GSM-NDVI (a) and AM-NDVI (b) over the Loess Plateau. Slopes of the periods of last three decades (1982–2015), before the GGP (1982–1999), and after the GGP (1999–2015) were also shown. * indicates the trend is not significant ($p > 0.05$).

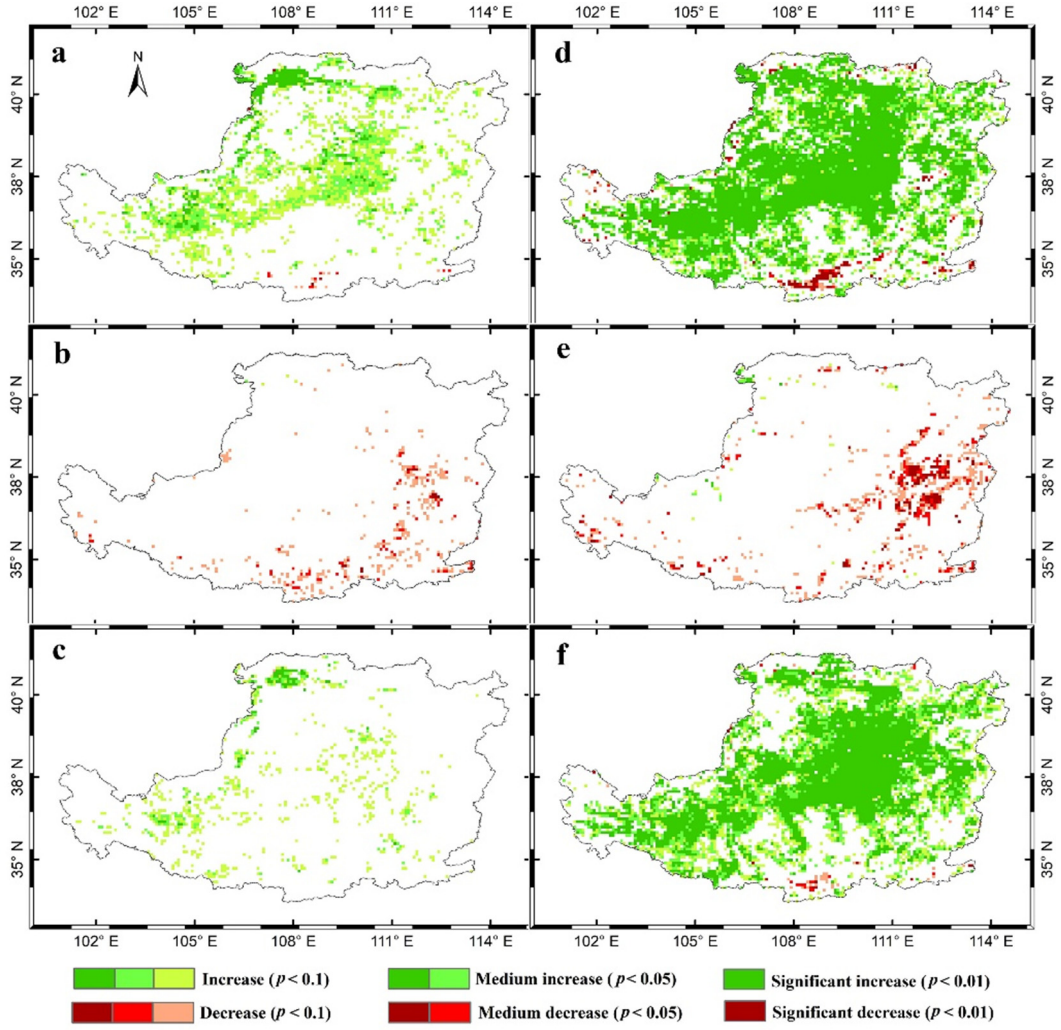

Fig. 4. The change levels of GSM-NDVI and AM-NDVI during the periods of 1982–2015 (a and d), before the GGP (b and e), and after the GGP (c and f), respectively. The nodata pixels indicate the changes of NDVI were not significant ($p > 0.1$).

were mostly found in northern, central, and western LP. The increasing GSM-NDVI were mainly distributed in regions in central, western, and northern LP.

3.3. Correlations between NDVI and the climate related variables

To analyze the relationships between NDVI and the variables related to climate, in the first step, the anomalies of their spatially averaged data were compared (Fig. S2). The pattern of AM-NDVI was similar to that of GSM-NDVI, and showed larger inter-annual variation. The GSM-NDVI showed a more disciplinary inter-annual variation. The year-to-year variations in SEDI were very similar to those of NDVI, followed by RSM, precipitation, and temperature.

In addition, the slopes of NDVI and each climatic variable during each period were compared (Table 1). The results showed that the annual mean precipitation, temperature, and SEDI increased during 1982–2015, with slopes of 4.48×10^{-1} mm year^{-1}, 3.69×10^{-2} °C year^{-1}, and 7.45×10^{-3} year^{-1}, respectively, which is consistent with the variation of AM-NDVI (Fig. 3). In contrast, the annual mean RSM slightly decreased, with a slope of -2.97×10^{-3} year^{-1}. Consistent with the increasing GSM-NDVI, the mean precipitation, temperature, and SEDI during growing season were increasing, with slopes of 3.47×10^{-1} mm year^{-1}, 3.75×10^{-2} °C year^{-1}, and 3.11×10^{-3} year^{-1}, respectively. However, the corresponding RSM was decreasing, with a slope of -1.27×10^{-4} year^{-1}.

Before the GGP was launched in 1999, all the MAP, annual mean RSM, and SEDI were decreasing, with slopes of −2.68 mm year^{-1},

Table 1
Slopes of the climate related variables in the LP over the last decades.

Climate related variables	Annual			Growing-season		
	1982–1999	1999–2015	1982–2015	1982–1999	1999–2015	1982–2015
Precipitation (mm yr^{-1})	−2.68	4.24	4.48×10^{-1}	-5.12^{*}	3.09	3.47×10^{-1}
Temperature (°C yr^{-1})	$8.14 \times 10^{-2***}$	-2.28×10^{-2}	$3.69 \times 10^{-2***}$	$6.08 \times 10^{-2***}$	-2.73×10^{-3}	$3.75 \times 10^{-2***}$
RSM (% yr^{-1})	-5.93×10^{-4}	$1.05 \times 10^{-3**}$	-2.97×10^{-6}	-4.75×10^{-4}	$9.31 \times 10^{-4**}$	-1.27×10^{-4}
SEDI (yr^{-1})	-1.19×10^{-2}	$4.58 \times 10^{-2***}$	7.45×10^{-3}	-1.20×10^{-2}	$4.01 \times 10^{-2**}$	3.11×10^{-3}

*** Indicate $p < 0.01$.
** Indicate $p < 0.05$.
* Indicate $p < 0.1$.

-5.93×10^{-4} year^{-1}, and -1.19×10^{-2} year^{-1}, respectively. In contrast, the MAT was increasing at a rate of 8.14×10^{-2} °C year^{-1}. The mean precipitation, RSM, and SEDI during growing-season were decreasing with slopes of -5.12 mm year^{-1}, -4.75×10^{-2} year^{-1}, and -1.19×10^{-2} year^{-1}, respectively. The corresponding temperature increased with a slope of 6.08×10^{-2} °C year^{-1}. These results suggested that except human activities (e.g., deforestation) the decreasing precipitation, drying soil, and anabatic drought together exerted strong and negative impacts on the vegetation in the LP before the GGP was launched in 1999.

During the period after the GGP was launched, both annual and growing-season precipitation increased in the LP, with slopes of 4.24 mm year^{-1} and 3.09 mm year^{-1}, respectively. The corresponding temperature were slightly decreasing, with slopes of -2.28×10^{-2} °C year^{-1} and -2.73×10^{-2} °C year^{-1}, respectively. Accompanied with the increasing precipitation, the RSM and SEDI increased significantly. The annual and growing-season mean RSM significantly increased with slopes of 1.05×10^{-3} year^{-1} and 9.31×10^{-4} year^{-1} ($p < 0.05$), respectively. The corresponding SEDI showed significant increases with slopes of 4.58×10^{-2} year^{-1} ($p < 0.01$) and 4.01×10^{-2} year^{-1} ($p < 0.05$), respectively. These results indicated that not only the GGP (e.g., afforestation), but also climate changes (increasing precipitation, increasing RSM, and decreased SEDI) may produce large and positive impacts on the increasing NDVI in the LP for the duration of 1999–2015.

Fig. 5 shows the spatial distributions of the slopes of the NDVI and climatic variables over 1982–2015. The increasing NDVI of the central LP was identical to the increased precipitation, increased temperature,

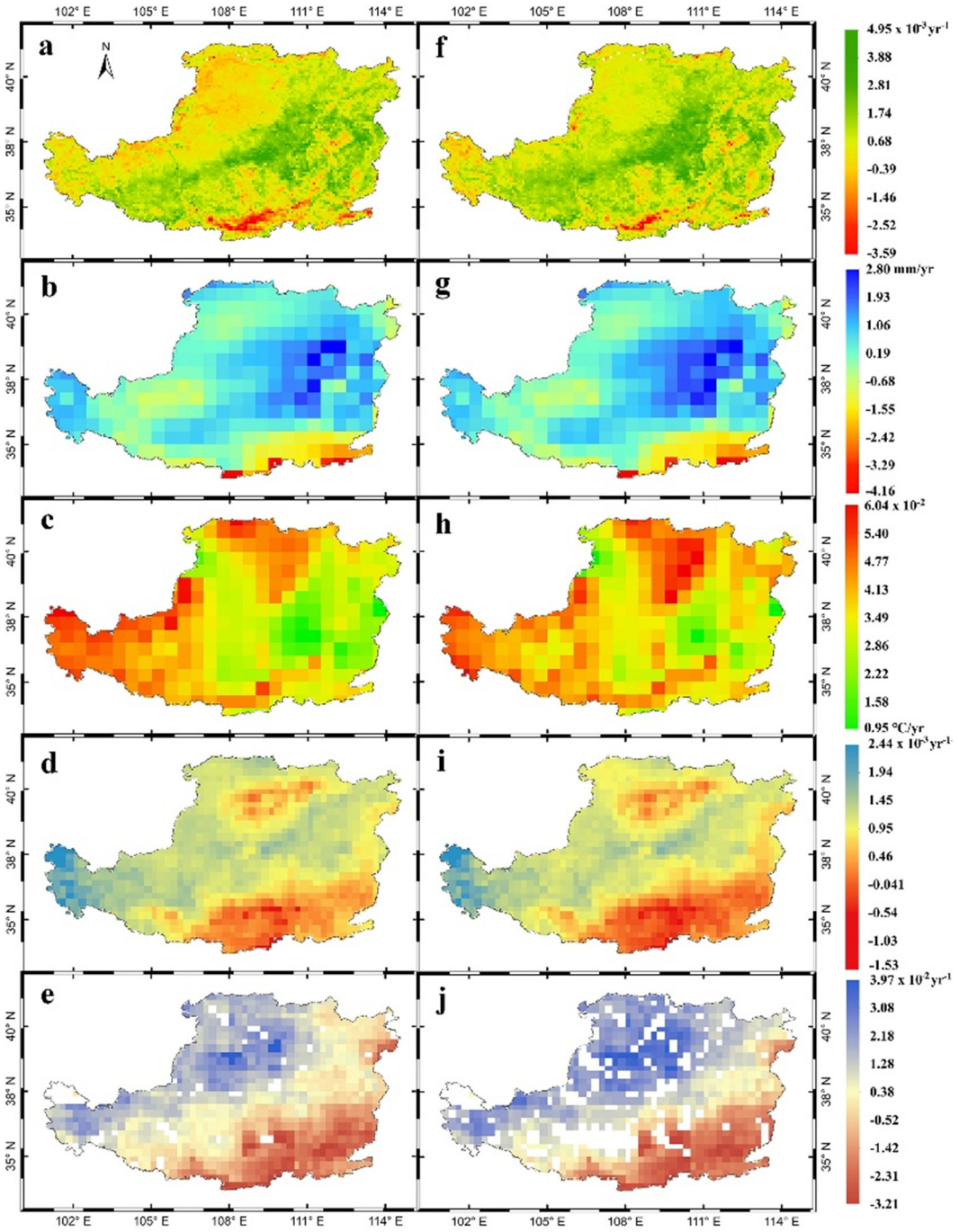

Fig. 5. Spatial distributions of the slopes of growing-season mean (a–e) and annual mean (f–j) NDVI, precipitation, temperature, root soil moisture, and SEDI in the LP over 1982–2015.

increased RSM, and reduced drought. In contrast, accompanied by the decreasing precipitation, relatively faster increase of temperature, decrease of RSM, and anabatic drought, both AM-NDVI and GSM-NDVI were significantly decreasing in the southern LP. In the southwestern LP, although this area showed no significant increases in precipitation, RSM, and SEDI, the NDVI significantly increased, suggesting that the GGP played dominant role in determining the NDVI dynamics. In the northwestern LP, although the precipitation slightly increased and the drought decreased, the GSM-NDVI was slightly decreasing. In contrast, the AM-NDVI showed a slight increase in the northwestern LP, indicating that the changes of GSM-NDVI were more sensitive to climate change.

During the period before the initiation of the GGP most regions of the LP experienced decreasing NDVI (Fig. S3). In particular, the GSM-NDVI of the forests in the southeastern and western LP was significantly decreasing, with slopes of less than -6.00×10^{-3} year^{-1}. For the croplands in the southern and eastern LP and the grasslands in the northwestern and western LP, the trends of GSM-NDVI ranged from 0 to -6.00×10^{-3} year^{-1}. The corresponding temperature increased significantly over the LP. The precipitation, RSM, and SEDI were significantly decreasing in the southern and southeastern LP, suggesting that the significantly decreasing NDVI in the southeastern and southern forested regions may be largely determined by the significantly decreasing water availability and rising temperature. In contrast, in the northwestern and western LP, no significant changes were found for precipitation, while the RSM and SEDI were slightly increasing, indicating that the slightly decreases in NDVI may mainly result from the significantly rising temperature. Compared to the GSM-NDVI, the decreasing magnitudes of AM-NDVI were relatively small in most regions of the LP. In addition, the AM-NDVI was slightly increasing in several regions in the northwestern and southern LP.

The spatial distributions of the trends of GSM-NDVI and AM-NDVI over 1999–2015 clearly showed that the GGP largely changed the vegetation of the LP (Fig. S4). The GSM-NDVI changed from decreases before GGP to increases in the central, southwestern, and eastern LP, with slopes larger than 2.0×10^{-3} year^{-1}. However, it continued to decrease in the northwestern, southern, and western LP. The spatial distributions of the corresponding precipitation, temperature, RSM, and SEDI suggest that the increasing precipitation, decreasing temperature, increasing RSM, and decreasing drought during the growing season in the central LP may accelerate the growth of vegetation. Although the RSM and SEDI were slightly increasing in the southwestern LP during growing season, the precipitation was not significantly changed and the temperature was clearly increasing. In the southern and northwestern LP, the GSM-NDVI were significantly decreasing, which was identical to the trends of corresponding precipitation, temperature, RSM, and drought. This result indicated that the decreasing GSM-NDVI in these regions was mainly caused by the negative effects of climate related variables. With the exception of several regions in the southern, western, and northwestern LP, most regions of the LP showed increasing AM-NDVI over 1999–2015. The trends of corresponding precipitation, temperature, RSM, and SEDI suggest that the increasing AM-NDVI may be largely determined by changes in the climatic variables in the central and eastern LP, while it may be mainly caused by the GGP in western and northern LP. The decreasing AM-NDVI in the southern LP is likely caused by the decreasing MAP, significantly increasing MAT, decreasing RSM, and anabatic drought.

3.4. Sensitivities of NDVI variations to climate related variables

The coefficients of multiple linear regression analyses were used to represent the sensitivities of the inter-annual variations of NDVI to climate related variables for each of the texted periods (Table 2). The results show that the corresponding inter-annual variations of the four variables (precipitation, temperature, RSM, and SEDI) explained 21% ($p = 0.14$) and 28% ($p = 0.04$) of the changes in AM-NDVI and GSM-NDVI during 1982–2015, respectively. The inter-annual variation of AM-NDVI positively correlated with each of the climate related variables. It was most sensitive to RSM, followed by temperature, precipitation, and SEDI, with sensitivities (i.e., absolute values of the regression coefficient) of 0.43, 0.35, 0.10, and 0.01, respectively. The inter-annual variation of GSM-NDVI positively correlated with that of RSM, precipitation, and temperature for 1982–2015, but negatively with SEDI. Its sensitivities to RSM, SEDI, precipitation, and temperature were 0.82, 0.53, 0.34, and 0.22 respectively. This result indicates that the changes in the GSM-NDVI in the LP for 1982–2015 were most sensitive to RSM, followed by drought, precipitation, and temperature. These analyses demonstrate that the vegetation in the LP was more sensitive to the RSM than to other variables at both annual and growing-season scales during the period of 1982–2015; it was more sensitive to drought and precipitation at the growing-season scale than at the annual scale, while it was more sensitive to temperature at the annual scale than at the scale of the growing -season.

The changes of the four variables explained 31% ($p = 0.26$) and 44% ($p = 0.09$) of the variations in the AM-NDVI and GSM-NDVI during the period before the GGP (1982–1999). Both the AM-NDVI and GSM-NDVI positively correlated with RSM and precipitation, while they correlated negatively with temperature and SEDI. The inter-annual variations of NDVI in the LP during 1982–1999 were most sensitive to RSM, followed by SEDI, with sensitivities of 1.03 and 0.95 for AM-NDVI as well as 1.42 and 1.24 for GSM-NDVI, respectively. In addition, the GSM-NDVI was more sensitive to temperature than the AM-NDVI, while it was less sensitive to precipitation.

During the period after the GGP was launched (1999–2015), the inter-annual variations of the NDVI could be explained well by the changes in the four climate related variables, with R^2 of 0.44 ($p = 0.12$) and 0.51 ($p = 0.05$) for AM-NDVI and GSM-NDVI, respectively. The inter-annual variation of AM-NDVI correlated positively with that of SEDI, temperature, and precipitation, with sensitivities of 0.91, 0.30, and 0.04, respectively, while it correlated negatively with the RSM, with a sensitivity of 0.25. The GSM-NDVI correlated positively with RSM, temperature, and precipitation, with sensitivity values of 1.00, 0.07, and 0.01, respectively, while correlated negatively with SEDI, with a sensitivity of 0.28. Compared to the period before the GGP, the sensitivity of NDVI to the increasing temperature (Table 1) changed from negative to positive; the sensitivity AM-NDVI to the SEDI changed from negative to positive, and that of GSM-NDVI decreased. These results indicate that during the period before the GGP was launched the climate changes (warming and drying, Table 1) exerted adverse effects on the vegetation in the LP. However, after the GGP was launched the wetting climate and the decreased drought yielded positive effects for the vegetation.

Furthermore, partial correlation analysis was used to analyze the effects of the inter-annual variation of each climate related variable on that of the NDVI at the pixel scale for 1982–2015. Fig. 6 shows that in

Table 2
Sensitivities of the inter-annual variations of NDVI to the climatic variables.

Periods	Regression coefficients (annual)					Regression coefficients (growing-season)				
	γ_{pre}	δ_{tem}	φ_{SM}	ψ_{SEDI}	R^2	γ_{pre}	δ_{tem}	φ_{SM}	ψ_{SEDI}	R^2
1982–2015	0.10	0.35	0.43	0.01	0.21	0.34	0.22	0.82	−0.53	0.28
1982–1999	0.26	−0.03	1.03	−0.95	0.31	0.11	−0.18	1.42	−1.24	0.44
1999–2015	0.04	0.30	−0.25	0.91	0.43	0.01	0.07	1.00	−0.28	0.51

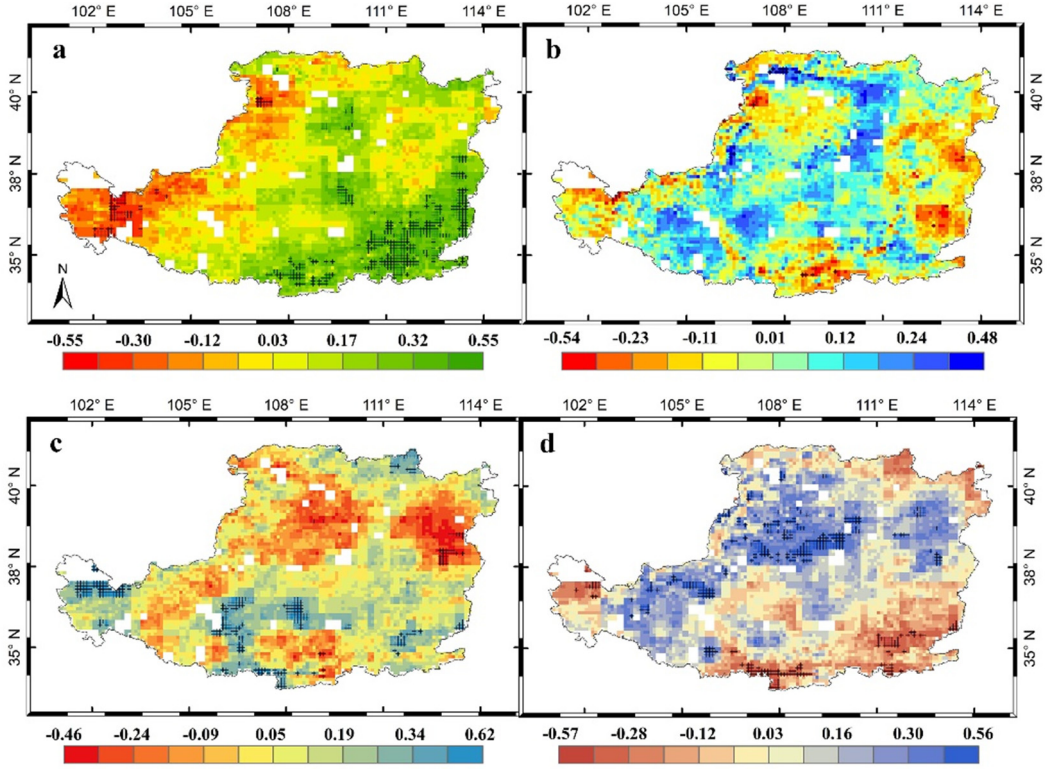

Fig. 6. Spatial distributions of the partial correlation coefficients between GSM-NDVI and precipitation (a), temperature (b), root-soil moisture (c), and SEDI (d), during 1982–2015 over the LP. The black cross indicates that the partial correlation coefficient was significant ($p < 0.05$).

the southeastern, western, and southern LP, the inter-annual variations of GSM-NDVI were mainly caused by precipitation. Temperature had obvious effects on NDVI in eastern, western, southwestern, and several regions in the southern and northern LP; however, these effects were not significant. The RSM significantly affected NDVI in the western and several regions in the southwestern LP, while the effects were not

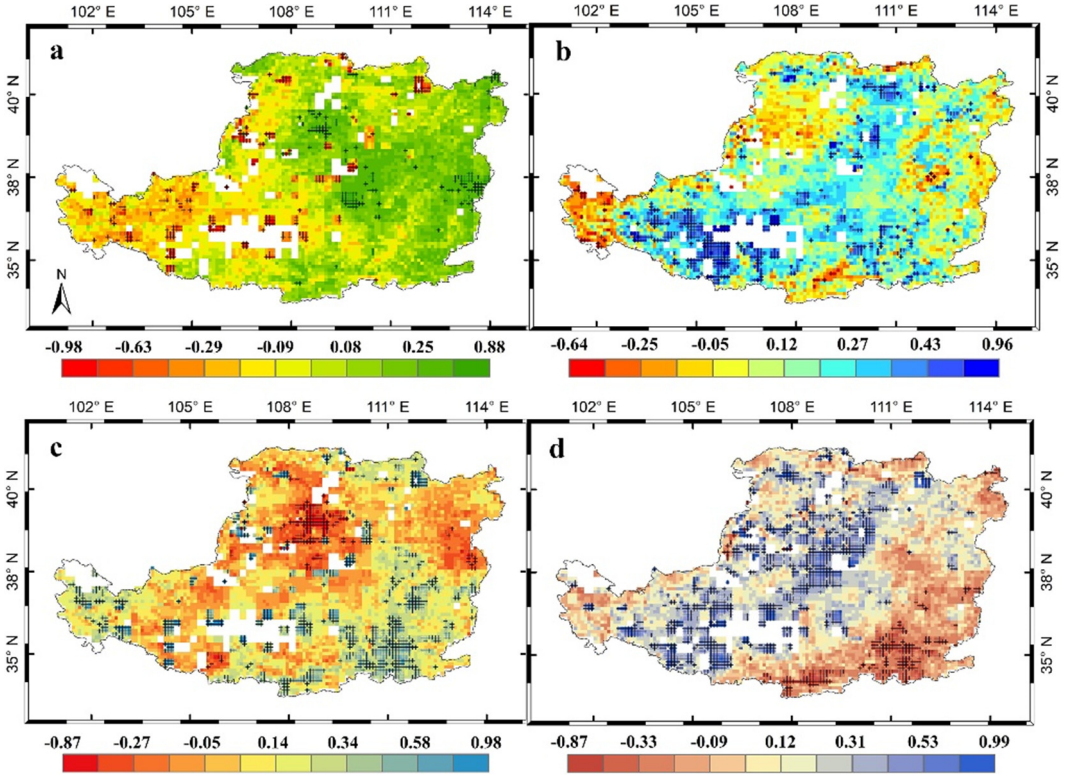

Fig. 7. Same as Fig. 6, but for AM-NDVI.

obvious in the other investigated regions. The SEDI significantly affected the NDVI in the northwestern LP and several regions in the southern and western LP, while the effects were small in the other regions.

Fig. 7 shows the spatial distributions of the partial correlation coefficients between AM-NDVI and the climatic variables. The results suggest that the inter-annual variations of precipitation exerted obvious effects on NDVI in the eastern, central, and western LP, but the effects were relatively small in the other investigated regions. The inter-annual variations of temperature significantly affected that of NDVI in the southwestern and several regions in the northern and southeastern LP, while it was not significant for the other investigated regions. The inter-annual variations of NDVI were significantly affected by that of RSM in several local regions in the southeastern, northwestern, and western LP, while it was primarily determined by other factors in the remaining regions. Fig. 7d clearly shows that the inter-annual variations of SEDI primarily determined the NDVI in most regions of the southeastern and northwestern LP, and several regions in southwestern LP. These results suggest that the inter-annual variations in the climate related variables significantly affected the AM-NDVI in the southeastern, southwestern, and northeastern LP for 1982–2015.

4. Discussion

Using long-term AVHRR-based NDVI data and several global or regional climatic data sets, vegetation changes in the LP were assessed over the last three decades; furthermore, the impacts of the GGP and climate changes on the NDVI were analyzed. The assessment showed that during the period before the GGP was launched (1982–1999), the spatially averaged AM-NDVI over the LP decreased, while it changed into a significant increase after the GGP (1999–2015). During the period of 1982–2015, it significantly increased. The trends of GSM-NDVI during the corresponding periods were consistent with AM-NDVI, but were not significant. These results suggest that the GGP project, which was launched in 1999, largely changed the vegetation dynamics in the LP. These results are also consistent with several previous studies (Xiao, 2014; Feng et al., 2016; Zhang et al., 2016; Li et al., 2017). For example, using the MODIS enhanced vegetation index (EVI) and LAI products Xiao (2014) assessed the vegetation changes in the LP over 2000–2013 and found that mean EVI and LAI during the growing season in the LP increased by 0.12 and 0.11 for this period, respectively. Feng et al. (2016) reported that the GGP caused a 25% increase in vegetation cover in the LP over the last decade. Zhang et al. (2016) reported that prior to the launch of the GGP in 1999, 73.3% of the LP showed no significant changes in AM-NDVI. However, after the launch of the GGP, most areas of the LP (82.4%) showed a significantly increasing AM-NDVI. This indicates that human activities exerted a larger impact on vegetation over the LP than climate change, at least for the period after the launch of the GPP. This inference was also consistent with recent studies based on process-based models (Gang et al., 2018; Li et al., 2018). In addition, the conducted analyses showed that both the spatially averaged AM-NDVI and GSM-NDVI had large inter-annual variations during the period of 1982–2015, suggesting that with the exception of human activities (deforestation or afforestation) the changes of climate also strongly affected the vegetation growth. Compared to AM-NDVI, the GSM-NDVI showed larger inter-annual variation (Fig. 3). A possible reason is that vegetation was more influenced by the climate related factors during the growing season. In addition, our analyses showed that the areas with significantly changed GSM-NDVI were much smaller than those of AM-NDVI (Fig. 4). This result highlights that analyses should be performed not only at the annual scale, but also at the growing-season scale, when land vegetation dynamics and their responses to climate change are to be quantified.

When investigating the impacts of climate change on NDVI in the LP, except for precipitation and temperature, the relationships between NDVI and RSM, and SEDI were also examined. The RSM and SEDI data sets were obtained from the GLEAM global RSM and SEDI products. It should be noted that they were not validated against measurements in this particular area, which was beyond the scope of this study. The intrinsic uncertainties of these data sets may partly affect the results of the conducted analyses. However, the wide use of these data in previous studies (Miralles and Teuling, 2014; Guillod et al., 2015; Vicente-Serrano et al., 2018) indicates that their ability to capture the spatio-temporal variations of soil moisture and drought at the regional scale.

Our analyses show that the NDVI, the annual mean precipitation, temperature, and SEDI were increasing during 1982–2015, while the RSM was decreasing. These results indicate that except for the GGP, the increasing precipitation, increasing temperature, and decreasing drought may also have significantly contributed to the increasing NDVI in the LP over the past three decades; although the reduced RSM may partly negatively impact the NDVI, its effects were relatively small (Table 1). In addition, our analyses suggest that the climate was warming and drying during the period before the GGP was launched (Table 1). The decreasing NDVI and its sensitivities to climatic variables (Table 2) during this period suggest that this synchronous drying and warming climate should have cause adverse effects on the vegetation. In contrast, the warming climate and decreased drought during the period after the GGP should contribute to the increasing NDVI. Although the temperature decreased during this period, the resulting effect on the NDVI was limited (Table 2).

The sensitivities of the inter-annual variations of the NDVI to the climatic variables were examined through multiple linear regression analyses. The results show that the variations of NDVI in the LP were most sensitive to that of RSM rather than the other climate related variables; the GGP project changed the responses of the variation of NDVI to the warming climate. In contrast to previous studies, our analyses highlight the importance of the impacts of RSM on the vegetation dynamics in this arid and semi-arid region, where the ecosystems are primarily limited by water availability. In addition, our analyses showed that, after the GGP was launched in 1999, although accompanied by an increasing precipitation, and the significantly increased NDVI in several regions of the LP, the RSM was not significantly changed, and the temperature increase was relatively small and even decreasing. These results are consistent with several previous studies (Feng et al., 2016; Zhang et al., 2017), suggesting that large-scale afforestation may have caused more water losses through transpiration and thus exerted a cooling effect.

5. Conclusion

In summary, the NDVI changes in the LP were assessed during last three decades, which included both the period before the GGP, and the period after the GGP. On base of the assessments, the correlations between NDVI and several environmental variables were analyzed. The major conclusions are as follows:

(1) The GGP greatly changed the vegetation in the LP since it was launched. Both the GSM-NDVI and AM-NDVI slightly decreased ($p < 0.05$) in the LP before the GGP launched in 1999; however, they became slightly and significantly increased after the GGP (1999–2015), respectively.
(2) Changes of climate, i.e., warming and drying, had adverse effects on vegetation in the LP during the period before the GGP was launched (1982–1999). In contrast, the changes (warming, wetting, and reduced drought) yielded positive effects during the period after the GGP (1999–2015).
(3) The inter-annual variations of NDVI in the LP were primarily determined by that of RSM rather than by precipitation or other climatic variables. The GSM-NDVI was far more sensitive to changes of climate than the AM-NDVI.
(4) In the southeastern LP, the inter-annual variations of the GSM-NDVI were mainly determined by that of precipitation and SEDI; in the northwestern LP these were primarily caused by SEDI and RSM; in the eastern and southwestern LP, these were

mainly determined by temperature and RSM. The inter-annual variations of AM-NDVI in the southeastern and northwestern LP were mainly caused by that of SEDI and RSM, but were primarily determined by the temperature in the southwestern LP.

In addition, the increased vegetation coverage of the LP may also considerably affect the regional climate. Regardless of the increasing precipitation, the soil moisture continued to decrease, and the temperature decreased due to the cooling effect caused by the increased vegetation (i.e., increasing transpiration). Future research should investigate this feedback between the increasing vegetation and regional climate.

Acknowledgments

The authors thank the GIMMS group for providing the AVHRR NDVI data, the China Meteorological Data Service Center for providing the China climate dataset, and the GLEAM datasets group for providing the root-soil moisture and SEDI data. This work was supported the by National Natural Science Foundation of China (41801061, 41501093); and the Fund Project of Shaanxi Key Laboratory of Land Consolidation (2018-JC17).

Appendix A. Supplementary data

Supplementary data to this article can be found online at https://doi.org/10.1016/j.scitotenv.2019.01.028.

References

Chen, P., Shang, J., Qian, B., Jing, Q., Liu, J., 2017. A new regionalization scheme for effective ecological restoration on the Loess Plateau in China. Remote Sens. 9, 1323. https://doi.org/10.3390/rs9121323.

Fang, J.Q., Xie, Z., 1994. Deforestation in preindustrial China: the Loess Plateau region as an example. Chemosphere 29, 983–999.

Feng, X., Fu, B., Piao, S., Wang, S., Ciais, P., Zeng, Z., et al., 2016. Revegetation in China's Loess Plateau is approaching sustainable water resource limits. Nat. Clim. Chang. 6, 1019–1022.

Forzieri, G., Alkama, R., Miralles, D.G., Cescatti, A., 2017. Satellites reveal contrasting responses of regional climate to the widespread greening of Earth. Science 356, 1180–1184.

Gang, C., Zhao, W., Zhao, T., Zhang, Y., Gao, X., Wen, Z., 2018. The impacts of land conversion and management measures on the grassland net primary productivity over the Loess Plateau, Northern China. Sci. Total Environ. 645, 827–836.

Guillod, B.P., Orlowsky, B., Miralles, D.G., Teuling, A.J., Seneviratne, S.I., 2015. Reconciling spatial and temporal soil moisture effects on afternoon rainfall. Nat. Commun. 6, 6443. https://doi.org/10.1038/ncomms7443.

Guo, J., Gong, P., 2016. Forest cover dynamics from Landsat time-series data over Yan'an city on the Loess Plateau during the Grain for Green Project. Int. J. Remote Sens. 37, 4101–4118.

Jin, Z., Wang, X., Zhang, X., 2017a. Dated deposition couplets link catchment erosion flux with storm discharge on the Chinese Loess Plateau. Acta Geochim. 36, 548–551.

Jin, Z., Liang, W., Yang, Y., Zhang, W., Yan, J., Chen, X., et al., 2017b. Separating vegetation greening and climate change controls on evapotranspiration trend over the Loess Plateau. Sci. Rep. 7, 8191. https://doi.org/10.1038/s41598-017-08477-x.

Kendall, M., 1975. Rank Correlation Methods. Charles Griffen, London (ISBN 195205723).

Li, Z., Zheng, F.L., Liu, W.Z., Flanagan, D.C., 2010. Spatial distribution and temporal trends of extreme temperature and precipitation events on the Loess Plateau of China during 1961–2007. Quat. Int. 226, 92–100.

Li, C., Qi, J., Yang, L., Wang, S., Yang, W., Zhu, G., et al., 2014. Regional vegetation dynamics and its response to climate change-a case study in the Tao River Basin in Northwestern China. Environ. Res. Lett. 9, 125003. https://doi.org/10.1088/1748-9326/9/12/125003.

Li, S., Yang, S., Liu, X., Liu, Y., Shi, M., 2015. NDVI-based analysis on the influence of climate change and human activities on vegetation restoration in the Shaanxi-Gansu-Ningxia Region, Central China. Remote Sens. 7, 11163–11182. https://doi.org/10.1007/10.1029/2004GL021649.

Li, J., Li, Z., Lü, Z., 2016. Analysis of spatiotemporal variations in land use on the Loess Plateau of China during 1986–2010. Environ. Earth Sci. 75, 997. https://doi.org/10.1007/s12665-016-5807-y.

Li, J., Peng, S., Li, Z., 2017. Detecting and attributing vegetation changes on China's Loess Plateau. Agric. For. Meteorol. 247, 260–270.

Li, J., Wang, Z., Lai, C., Wu, X., Zeng, Z., Chen, X., et al., 2018. Response of net primary production to land use and land cover change in mainland China since the late 1980s. Sci. Total Environ. 639, 237–247.

Liu, J., Tian, H., Liu, M., Zhuang, D., Melillo, J.F., Zhang, Z., 2005. China's changing landscape during the 1990s: large-scale land transformations estimated with satellite data. Geophys. Res. Lett. 32, L02405. https://doi.org/10.1029/2004GL021649.

Mann, H.B., 1945. Nonparametric tests against trend. Econometrica 13, 245–259.

Martens, B., Miralles, D.G., Lievens, H., van der Schalie, R., de Jeu, R.A.M., Fernández-Prieto, D., et al., 2017. GLEAM v3: satellite-based land evaporation and root-zone soil moisture. Geosci. Model Dev. 10, 1903–1925.

Miralles, D.G., Teuling, A.J., 2014. Mega-heatwave temperatures due to combined soil desiccation and atmospheric heat accumulation. Nat. Geosci. 7, 345–349.

Piao, S., Sitch, S., Ciais, P., Friedlingstein, P., Peylin, P., Wang, X., et al., 2013. Evaluation of terrestrial carbon cycle models for their response to climate variability and to CO_2 trends. Glob. Chang. Biol. 19, 2117–2132.

Song, X.P., Hansen, M.C., Stehman, S.V., Potapov, P.V., Tyukavina, A., Vermote, E.F., et al., 2018. Global land change from 1982 to 2016. Nature 560, 639–643.

Sun, S., Song, Z., Wu, X., Wang, T., Wu, Y., Du, W., et al., 2018. Spatio-temporal variations in water use efficiency and its drivers in China over the last three decades. Ecol. Indic. 94, 292–304.

Tong, X., Brandt, M., Yue, Y., Horion, S., Wang, K., Keersmaecker, W.D., et al., 2018. Increased vegetation growth and carbon stock in China karst via ecological engineering. Nat. Sustain. 1, 44–50.

Tucker, C.J., Pinzon, J.E., Brown, M.E., Slayback, D.A., Pak, E.W., Mahoney, R., et al., 2005. An extended AVHRR 8–km NDVI dataset compatible with MODIS and SPOT vegetation NDVI data. Int. J. Remote Sens. 26, 4485–4498.

Vicente-Serrano, S.M., Miralles, D.G., Domínguez-Castro, F., Azorin-Molina, C., El Kenawy, A., McVicar, T.R., et al., 2018. Global assessment of the standardized evapotranspiration deficit index (SEDI) for drought analysis and monitoring. J. Clim. 31, 5371–5393.

Wang, S., Fu, B., Piao, S., Lü, Y., Ciais, P., Feng, X., et al., 2017a. Reduced sediment transport in the Yellow River due to anthropogenic changes. Nat. Geosci. 9, 38–41.

Wang, X., Wang, T., Liu, D., Guo, H., Huang, H., Zhao, Y., 2017b. Moisture-induced greening of the South Asia over the past three decades. Glob. Chang. Biol. 23, 4995–5005.

Wang, Y., Kang, M., Zhao, M., Xing, K., Wang, G., Xue, F., 2017c. The spatiotemporal variation of tree cover in the Loess Plateau of China after the 'Grain for Green' Project. Sustainability 9, 739. https://doi.org/10.3390/su9050739.

Xiao, J., 2014. Satellite evidence for significant biophysical consequences of the "Grain for Green" Program on the Loess Plateau in China. J. Geophys. Res. Biogeosci. 119, 2261–2275.

Yang, Z., Dong, J., Liu, J., Zhai, J., Kuang, W., Zhao, G., et al., 2017. Accuracy assessment and inter-comparison of eight medium resolution forest products on the Loess Plateau, China. ISPRS Int. J. Geogr. Inf. Sci. 6, 152. https://doi.org/10.3390/ijgi6050152.

Yuan, W., Li, X., Liang, S., Cui, X., Dong, W., Liu, S., et al., 2014. Characterization of locations and extents of afforestation from the Grain for Green Project in China. Remote Sens. Lett. 5, 221–229.

Zhang, B., Zhao, X., Jin, J., Wu, P., 2015. Development and evaluation of a physically based multiscalar drought index: the Standardized Moisture Anomaly Index. J. Geophys. Res. Atmos. 120 (575–511).

Zhang, B., He, C., Burnham, M., Zhang, L., 2016. Evaluating the coupling effects of climate aridity and vegetation restoration on soil erosion over the Loess Plateau in China. Sci. Total Environ. 539, 436–449.

Zhang, S., Yang, D., Yang, Y., Piao, S., Yang, H., Lei, H., et al., 2017. Excessive afforestation and soil drying on China's Loess Plateau. J. Geophys. Res. Biogeosci. 123, 923–935.

Zhao, G., Mu, X., Wen, Z., Wang, F., Gao, P., 2013. Soil erosion, conservation, and eco-environment changes in the Loess Plateau of China. Land Degrad. Dev. 24, 499–510.

Zhao, A., Zhang, A., Cao, S., Liu, X., Liu, J., Cheng, D., 2018. Responses of vegetation productivity to multi-scale drought in Loess Plateau, China. Catena 163, 165–171.

Zheng, F.L., 2006. Effect of vegetation changes on soil erosion on the Loess Plateau. Pedosphere 16, 420–427.

Zheng, F., He, X., Gao, X., Zhang, C., Tang, K., 2005. Effects of erosion patterns on nutrient loss following deforestation on the Loess Plateau of China. Agric. Ecosyst. Environ. 108, 85–97.